ELECTROMAGNETIC SCATTERING FROM A MULTILAYERED CYLINDER ARBITRARILY LOCATED IN A GAUSSIAN BEAM, A NEW RECURSIVE ALGORITHMS

Z. Wu and L. Guo

Department of Physics
Xidian University
Xi'an, Shannxi Province 710071
P. R. China

1. INTRODUCTION

In the recent years, the problem of scattering of an off-axis Gaussian beam by a multilayered cylinder has been the subject of extensive investigations since a great variety of practical scatters can be modeled

by a suitable arrangement of cylinders. This paper deals with the computation of electromagnetic scattering of a multilayered cylinder illuminated normally by a Gaussian beam.

Previous works include the scattering of a multilayered cylinder by a plane wave [1–5] and the scattering of a Gaussian beam by a conducting or a homogeneous dielectric cylinder.They assume that the radius of the cylinder was small enough with respect to the beam width and a collimated beam was also used [6–8]. Kozaki gave a more simpler expression of the scattering of a Gaussian beam by a homogeneous dielectric cylinder by considering amplitude and phase distribution [9]. Zimmermann et al. investigate the scattering of an off-axis 2D Gaussian beam by a homogeneous dielectric cylinder theoretically and experimentally [10]. Nevertheless the expressions of the beam shape coefficients are not proposed in detail. Yokota et al. and Ren et al. use the wave functions for anisotropic media and the complex point source expression of a Gaussian beam to analyze the scattering by an anisotropic-coated conducting cylinder [11–12]. This paper presents a rigorous analysis to the problem of scattering of an off-axis 2D Gaussian beam by a multilayered cylinder. Our approach is based on the exact solution of the Helmholtz equation in circular cylindrical coordinates. At the first-order approximation, the beam shape coefficients are determined more accurately. An iterative algorithm to compute the scattering of a Gaussian beam by a multilayered cylinder is obtained.These results provide an extension of our previous paper [3]. Our recursive formulae overcome the difficulties in computing Bessel functions when the size parameter of the multilayered cylinder becomes large. The numerical results are in good agreement with the limit cases when the multilayered cylinder is reduced to a homogeneous cylinder or when the Gaussian beam is reduced to the plane wave. Our algorithms can also be applicable to the microwave, milimeter range.

The paper is organized as follows. Sec. 2 describe the cylindrical Gaussian beam expansions in terms of plane wave spectrum and the vector cylindrical harmonics, respectively. In this section we also discuss the behaviours of the cylindrical beam shape coefficients. In Sec. 3, the characteristic of our algorithms are underlined for scattering of a multilayered cylinder illuminated by an off-axis Gaussian beam. A particular attention is devoted to the computation domain of the recursive algorithms. Numerical examples, which demonstrate the new recursive algorithms, are presented in Sec. 4. Sec. 5 gives some conclusion.

2. THEORETICAL ANALYSIS

(A) Cylindrical Gaussian Beam Expansion in terms of Plane Wave Spectrum
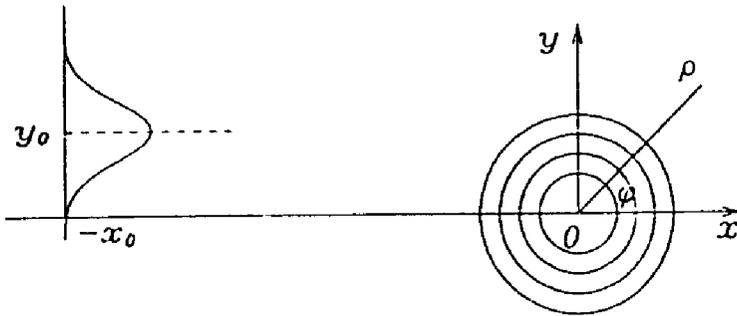

Figure 1. Geometry for the scattering of an off-axis incident Gaussian beam by a multilayered cylinder.

For the sake of simplicity, we consider the two dimensional (2D) problem which is displayed in Fig. 1. In this case, the incident beam propagates in the positive x-direction. If the electric field is polarised parallelly to the cylinder axis (z-axis), the magnetic field is transverse to the z-axis (TM case). If the electric field is perpendicularly polarised to the cylinder axis, the magnetic field is parallel to the z-axis (TE case). The time variation $e^{-i\omega t}$ has been assumed and suppressed. The wave number is equal to $k = 2\pi/\lambda$, where λ is the wavelength of the incident wave in free space. We also assume that the cylindrical Gaussian beam has its focal point located at $(-x_0, y_0)$. For TM case the electric field has only a z component. The spatial distribution of the amplitude E_z in the $x = x_0$ plane is given by

$$E_z(-x_0, y, z) = E_0 \exp\left[-\frac{(y-y_0)^2}{W_0^2}\right]$$

$$E_y(-x_0, y, z) = 0 \tag{1}$$

in which W_0 is the beam waist radius, the field components in Cartesian coordinates can be expanded in an angular spectrum of plane waves.

$$E_x(x, y, z) = \int_{-\infty}^{\infty} A_x(p, q) \exp[ik(px + qy)]dq$$

$$E_y(x, y, z) = \int_{-\infty}^{\infty} A_y(p, q) \exp[ik(px + qy)]dq \qquad (2)$$

$$E_z(x, y, z) = \int_{-\infty}^{\infty} A_z(p, q) \exp[ik(px + qy)]dq$$

with $p^2 + q^2 = 1$.

The complex amplitude of the plane waves A_x, A_y and A_z are determined from electric field components in the plane $x = -x_0$ which read as

$$
\begin{aligned}
A_z(p, q) &= \frac{1}{\lambda} \int_{-\infty}^{\infty} E_z(-x_0, y, z) \exp[-ik(px + qy)]dy \\
&= \frac{E_0\sqrt{\pi}W_0}{\lambda} \exp[-\frac{1}{4}k^2 W_0^2 q^2] \exp(ikpz_0 - ikqy_0) \qquad (3)
\end{aligned}
$$

Similarly, we can get $A_y(p, q) = 0$. According to the Maxwell equation, $\nabla \cdot \vec{E} = 0$, we obtain

$$pA_x + qA_y + \frac{\partial A_z}{\partial z} = 0$$

Taking into account relation (3), we have $\partial E_z/\partial z = 0$, including $A_x(p, q) = 0$, so that

$$E_x(x, y, z) = 0, \qquad E_y(x, y, z) = 0$$

$$
\begin{aligned}
E_z(x, y, z) = &\frac{E_0\sqrt{\pi}W_0}{\lambda} \int_{-\infty}^{\infty} \exp\left[-\frac{1}{4}k^2 W_0^2 q^2\right] \\
&\exp\left[ikp(x + x_0) + ikq(y - y_0)\right]dq \qquad (4)
\end{aligned}
$$

where E_z satisfies the Helmholtz equation

$$(\nabla^2 + k^2)E_z(x, y, z,) = 0 \qquad (5)$$

According to the Maxwell equations in a homogeneous isotropic medium, the components of magnetic fields yields

$$H_y = -\frac{1}{i\omega\mu}\frac{\partial E_z}{\partial x} = -\frac{kp}{\omega\mu}E_z \tag{6}$$

$$H_x = \frac{1}{i\omega\mu}\frac{\partial E_z}{\partial y} = \frac{kq}{\omega\mu}E_z \tag{7}$$

Obviously, the components of the magnetic field also satisfy the Helmholtz equation

$$(\nabla^2 + k^2)H_y = 0, \qquad (\nabla^2 + k^2)H_x = 0 \tag{8}$$

(B) The Expansion of the Electric and Magnetic Fields in Vector Cylindrical Harmonics

Let $x = \rho\cos\varphi$, $y = \rho\sin\varphi$, $p = \cos\gamma$, $q = \sin\gamma$ be the terms in the exponential of equation (4), we obtain

$$\exp\left[-\frac{1}{4}k^2W_0^2q^2 + ikp(x+x_0) + ikq(y-y_0)\right]$$
$$= \exp\left[-\frac{1}{4}k^2W_0^2q^2 + ikpx_0 - ikqy_0 + ik\rho\cos(\varphi-\gamma)\right]$$

According to

$$\exp\left[ik\rho\cos(\varphi-\gamma)\right] = \sum_{n=-\infty}^{\infty} i^n J_n(k\rho)e^{in(\varphi-\gamma)} \tag{9}$$

The electric field component E_z in cylindrical coordinates can be expressed as

$$E_z(x,y,z) = E_z(\rho,\varphi,z) = \frac{E_0\sqrt{\pi}W_0}{\lambda}\sum_{n=-\infty}^{\infty} i^n J_n(k\rho)e^{in\varphi}$$
$$\int_{-\infty}^{\infty} \exp\left[-\frac{1}{4}k^2W_0^2q^2 + ikpx_0 - ikqy_0 - in\gamma\right]dq \tag{10}$$

On the other way, E_z can also be expanded in cylindrical harmonics

$$E_z(\rho, \varphi, z) = E_0 \sum_{n=-\infty}^{\infty} C_n i^n J_n(k\rho) e^{in\varphi} \tag{11}$$

where $C_n (n = 0, \pm 1, \pm 2, ...)$ are the beam shape coefficients. Identifying (10) with (11), one may find that

$$C_n = \frac{\sqrt{\pi}W_0}{\lambda} \int_{-\infty}^{\infty} \exp\Big[-\frac{1}{4}k^2 W_0^2 q^2 + ik\sqrt{1-q^2}x_0$$
$$- ikqy_0 - in\sin^{-1}q \Big] dq \tag{12}$$

where $p = \sqrt{1-q^2}$, $\gamma = \sin^{-1}q$. The components of the magnetic field in cylindrical coordinates can also be derived in the similar way

$$H_\varphi = H_y \cos\varphi - H_x \sin\varphi$$
$$= -\frac{H_0\sqrt{\pi}W_0}{\lambda} \int_{-\infty}^{\infty} \cos(\varphi - \gamma)$$
$$\exp\Big[-\frac{1}{4}k^2 W_0^2 q^2 + ikpx_0 - ikqy_0 + ik\rho\cos(\varphi-\gamma) \Big] dq$$
$$= \frac{iH_0\sqrt{\pi}W_0}{\lambda} \sum_{n=-\infty}^{\infty} i^n J_n'(k\rho) e^{in\varphi}$$
$$\int_{-\infty}^{\infty} \exp\Big[-\frac{1}{4}k^2 W_0^2 q^2 + ikpx_0 - ikqy_0 - in\gamma \Big] dq$$
$$= iH_0 \sum_{n=-\infty}^{\infty} C_n i^n J_n'(k\rho) e^{in\varphi} \tag{13}$$

where the prime denotes differentiation with respect to the argument and

$$H_\rho = H_x \cos\varphi + H_y \sin\varphi$$
$$= \frac{H_0\sqrt{\pi}W_0}{\lambda} \int_{-\infty}^{\infty} (\sin\gamma\cos\varphi - \cos\gamma\sin\varphi)$$
$$\exp\Big[-\frac{1}{4}k^2 W_0^2 q^2 + ikpx_0 - ikqy_0 + ik\rho\cos(\varphi-\gamma) \Big] dq$$

$$= \frac{H_0\sqrt{\pi}W_0}{\lambda}\frac{1}{ik\rho}\sum_{n=-\infty}^{\infty}ini^n J_n(k\rho)e^{in\varphi}$$

$$\int_{-\infty}^{\infty}\exp\left[-\frac{1}{4}k^2W_0^2q^2+ikpx_0-ikqy_0-in\gamma\right]dq$$

$$= H_0\sum_{n=-\infty}^{\infty}C_n i^n\frac{J_n(k\rho)}{k\rho}e^{in\varphi} \tag{14}$$

Similarly to the case of a plane wave, the incident cylindrical Gaussian beam can be rewritten in vector cylindrical harmonics

$$\vec{E}_i = \sum_{n=-\infty}^{\infty}E_n C_n\vec{N}_n^{(1)} \tag{15}$$

$$\vec{H}_i = -\frac{ik}{\omega\mu}\sum_{n=-\infty}^{\infty}E_n C_n\vec{M}_n^{(1)} \tag{16}$$

where $E_n = i^n E_0/k$ for normal incidence and

$$\vec{N}_n^{(1)} = kJ_n(k\rho)e^{in\varphi}\hat{z} \tag{17}$$

$$\vec{M}_n^{(1)} = -\frac{dJ_n(k\rho)}{d\rho}e^{in\varphi}\hat{\varphi} + \frac{in}{\rho}J_n(k\rho)e^{in\varphi}\hat{\rho} \tag{18}$$

In the above discussions, we only consider the TM case. The solutions for the TE case can also be obtained.

(C) Beam Shape Coefficient

Terms ρ and γ of expression (12) can be expanded in Taylor series as

$$p = (1-q^2)^{\frac{1}{2}} = 1 - \frac{q^2}{2} + \cdots$$

$$\gamma = \sin^{-1}q = q + \frac{1}{6}q^3 + \cdots$$

If we choose $\gamma = q$, expression (12) can be rewritten for the lowest-order approximation as follows

$$C_{n0} = \frac{\sqrt{\pi}W_0}{\lambda} e^{ikx_0} \int_{-\infty}^{\infty} \exp\Big[-\frac{1}{4}k^2W_0^2q^2 - ikx_0\frac{q^2}{2} - ikqy_0 - inq\Big]dq$$

$$= \frac{\sqrt{\pi}W_0}{\lambda} e^{ikx_0} \int_{-\infty}^{\infty} \exp\Big[-\frac{1}{4}k^2W_0^2q^2(1 + i\frac{2x_0}{kW_0})q^2$$

$$- i(ky_0 + n)q\Big]dq \tag{19}$$

by introducing

$$l = kW_0^2, \quad Q_0 = (i - \frac{2x_0}{l})^{-1}, \quad s = \frac{1}{kW_0}, \quad \beta_n = ky_0 + n$$

The equation (19) can be formulated as

$$C_{n0} = \frac{\sqrt{\pi}W_0}{\lambda} e^{ikx_0} \int_{-\infty}^{\infty} \exp\Big[-\frac{1}{4}k^2W_0^2q^2 - i\beta_n q\Big]dq$$

$$= e^{ikx_0}\sqrt{iQ_0}\exp\Big[-iQ_0\frac{(ky_0 + n)^2}{W_0^2}\Big] \tag{20}$$

If we choose $\gamma = \sin^{-l} q = q + \frac{1}{6}q^3$, by ignoring the terms of higher orders, equation (12) can be approximated by

$$C_{n1} = \Big[1 + (\frac{n}{6})(s\sqrt{2iQ_0})^3(z^3 - 3z)\Big]C_{n0} \tag{21}$$

where $z = s\sqrt{2iQ_0}(n + ky_0)$. In Fig. 2, we give some examples of computational results of beam shape coefficients from (20) and (21).

In Fig. 2(a), the beam shape coefficients for the lowest-order and the first-order approximation are displayed in the case of the on-axis Gaussian beam. It is obvious that the oscillations decrease with increasing value of n for both C_{n0} and C_{n1}. As n increases enough, the real part and imaginary part tend to converge to the same zero value. Fig. 2(b) gives the comparison of the beam shape coefficients with first-order approximation for different x_0 value. We obtain the similar conclusion that longer distance between Gaussian beam and the cylinder is, the larger oscillation of C_n for the small value of n. With increasing of n, each curve converges to zero. We also consider
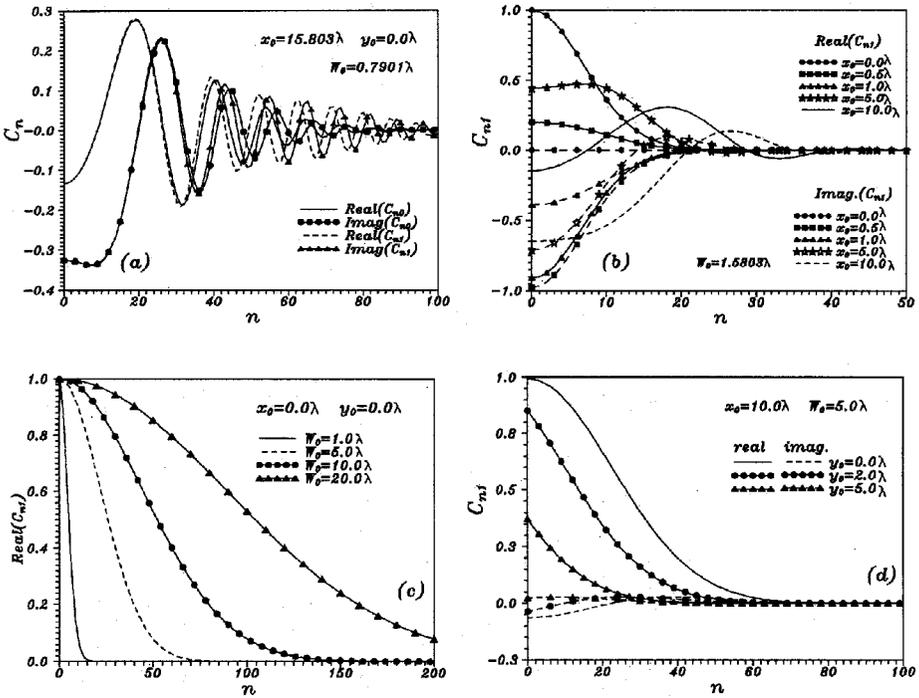
Figure 2. Beam shape coefficients versus n.

the beam shape coefficients for different beam width W_0 in Fig. 2(c). It should be noticed that as W_0 becomes larger with respect to the outer radius of the multilayered cylinder, the beam shape coefficients decrease more slowly to zero with increasing of n. The computed results of beam shape coefficients in the case of an off-axis Gaussian beam is displayed in Fig. 2(d). It gives the beam shape coefficients versus different y_0. Similarly to the previous case (Figs. 2(a), 2(b) and 2(c)), C_n also converges to the exact zero value with increasing of n. With larger y_0, the curves converge more quickly to zero.

3. THE ALGORITHM OF THE SCATTERING COEFFI-CIENTS

(A) Computation of Scattering Coefficients for Multilayered Cylinders

Let the axis of the multilayered cylinder be parallel to the z-axis. The cylinder is illuminated by an off-axis Gaussian beam at normal which is shown in Fig. 1. r_j is the radius of the j-th region of the multilayered cylinder. The corresponding size parameter is $x_j = k_0 r_j = 2\pi r_j/\lambda$. The relative refractive index and the characteristic impedance are m_j and η_j, respectively. The incident field, scattering field and the interior field in each region of the multilayered cylinder can be expanded in terms of cylindrical harmonic functions. For TM case we obtain

$$\vec{E}_s = - \sum_{n=-\infty}^{\infty} E_n(b_{nI}\vec{N}_n^{(3)} + ia_{nI}\vec{M}_n^{(3)}) \tag{22}$$

$$\vec{H}_s = \frac{ik}{\omega\mu} \sum_{n=-\infty}^{\infty} E_n(b_{nI}\vec{M}_n^{(3)} + ia_{nI}\vec{N}_n^{(3)}) \tag{23}$$

$$\vec{E}_j = \sum_{n=-\infty}^{\infty} E_n(c_n^{(j)}\vec{M}_n^{(1)} + d_n^{(j)}\vec{N}_n^{(1)} + g_n^{(j)}\vec{M}_n^{(2)} + f_n^{(j)}\vec{N}_n^{(2)}) \tag{24}$$

$$\vec{H}_j = -\frac{ik_j}{\omega\mu_j} \sum_{n=-\infty}^{\infty} E_n(c_n^{(j)}\vec{N}_n^{(1)} + d_n^{(j)}\vec{M}_n^{(1)} + g_n^{(j)}\vec{N}_n^{(2)} + f_n^{(j)}\vec{M}_n^{(2)}) \tag{25}$$

According to the boundary conditions and the radiation condition, one can set up two independent sets of simultaneous equations with unknown coefficients $a_{nI}, b_{nI}, c_n^{(j)}, d_n^{(j)}, f_n^{(j)}, g_n^{(j)}, (j = 1, 2, ..., t)$. Solving these equations, the scattering coefficients $a_{nI} = 0$ and b_{nI} can also be obtained. It is noticed that these equations can not be separated into two independent sets for an oblique incident. Similar to our previous paper [3], the scattering coefficients can be obtained as following for a Gaussian beam incidence.

According to $A_n^{(j)} = g_n^{(j)}/d_n^{(j)}$ and $B_n^{(j)} = f_n^{(j)}/c_n^{(j)}$, we obtain $A_n^{(1)} = B_n^{(1)} = 0$. Because $g_n^{(1)} = f_n^{(1)} = 0$, the coefficient b_{nI} can be eventually transformed into simple and suitable calculational forms. The recursing formulae can be written as follows

$$B_n^{(1)} = 0 \quad , \quad H_n^b(m_1 x_1) = D_n^{(1)}(m_1 x_1) \tag{26}$$

$$B_n^{(j)} = \frac{J_n(m_j x_{j-1})}{Y_n(m_j x_{j-1})} \cdot \frac{\eta_{j-1} D_n^{(1)}(m_j x_{j-1}) - \eta_j H_n^b(m_{j-1} x_{j-1})}{\eta_{j-1} D_n^{(2)}(m_j x_{j-1}) - \eta_j H_n^b(m_{j-1} x_{j-1})} \tag{27}$$

$$H_n^b(m_j x_j) = \frac{J_n(m_j x_j)/Y_n(m_j x_j) \cdot D_n^{(1)}(m_j x_j)}{J_n(m_j x_j)/Y_n(m_j x_j) - B_n^{(j)}} \\ - \frac{B_n^{(j)} D_n^{(2)}(m_j x_j)}{J_n(m_j x_j)/Y_n(m_j x_j) - B_n^{(j)}} \tag{28}$$

$$b_{nI} = C_{n1} \cdot \frac{J_n(x_t)}{H_n^{(1)}(x_t)} \cdot \frac{\eta_t D_n^{(1)}(x_t) - H_n^b(m_t x_t)}{\eta_t D_n^{(3)}(x_t) - H_n^b(m_t x_t)} \tag{29}$$

By exchanging the impedances η_{j-1} and η_j in (27),(29) and by replacing $B_n^{(j)}$ with $A_n^{(j)}$ and $H_n^b(m_j x_j)$ with $H_n^a(m_j x_j)$, the scattering coefficient a_{nII} for TE wave is expressed as

$$a_{nII} = C_{n1} \cdot \frac{J_n(x_t)}{H_n^{(1)}(x_t)} \cdot \frac{D_n^{(1)}(x_t) - \eta_t H_n^a(m_t x_t)}{D_n^{(3)}(x_t) - \eta_1 H_n^a(m_t x_t)} \tag{30}$$

This procedure involves only three logarithmic derivatives of Bessel functions. $D_n^{(1)}(z) = J_n'(z)/J_n(z)$, $D_n^{(2)}(z) = Y_n'(z)/Y_n(z)$, $D_n^{(3)}(z) = H_n^{(1)'}(z)/H_n^{(1)}(z)$, and the ratio $J_n(z)/Y_n(z)$. For function $D_n^{(1)}(z)$, the downward recurrence relation

$$D_{n-1}^{(1)}(z) = (n-1)/z - [D_n^{(1)}(z) + n/z]^{-1} \tag{31}$$

is used. $D_n^{(2)}(z)$, $D_n^{(3)}(z)$ and $J_n(z)/Y_n(z)$ are computed by using upward recurrence relation

$$D_n^{(2,3)}(z) = n/z - [(n-1)/z - D_{n-1}^{(2,3)}(z)]^{-1} \tag{32}$$

with

$$\frac{J_n(z)}{Y_n(z)} = \frac{J_{n-1}(z)}{Y_{n-1}(z)} \cdot \frac{[D_n^{(2)}(z) + n/z]}{[D_n^{(1)}(z) + n/z]} \tag{33}$$
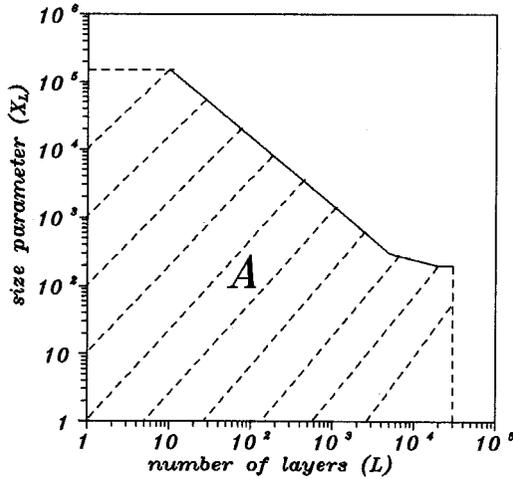
Figure 3. Computation domain in logarithmic scale.

(B) Computational Domain

In applications of light scattering to fibers sizing, fiber with considerable large size and a continues variation of the refractive index are encountered. The stratified cylinder model can successfully simulate any realistic inhomogeneous fiber. Naturally, it is very difficult to extensively compare the advantages and limitations of different recursive scheme. To test the computational domains, the profile of the refractive index is described by $n_i = n_1 + 0.5(n_L - n_1)(1 - \cos t\pi)$, and $n_1 = 1.01 n_L$, $n_L = 1.33$, $t = (i - 1)/(L - 1)$ and the size parameter are set to be $x_i = x_1 + t(x_L - x_1)$, $x_1 = 0.001 x_L$, $(i = 1, 2, 3, ..., L)$. In Fig. 3, the the computation domain (A) defines the possibilities of our algorithm results which was implemented as a FORTRAN LF90 code running on a PC 486/DX2. The program runs on the computer under the MS-DOS 6.2 operating system. In this figure, the number of layers versus the size parameters is displayed in logarithmic scales. Obviously, the electromagnetic scattering by a multilayered cylinder, whose number of layers is more than 30000 and the size parameter is more than 150000. Thus our new recursive algorithms overcome the previous difficulty in computing the scattering coefficients for inhomogeneous cylinders (including fibers, water jet, etc.) with large size parameters. As our computational method is based on discrete layers

when working on cylinders with a continuous gradient of refractive index. The question is: how many layers must be chosen to ensure an accurate solution for a given size? Since the backscattering coefficient is highly sensitive to the numbers of layers for a large, inhomogeneous and transparent cylinder, hence the numbers of layers can be easily got as the backscattering coefficient tends to be a constant.

4. NUMERICAL RESULTS AND DISCUSSIONS

The scattering fields and internal fields can be immediately obtained from equations (22)–(25) by inserting expressions (21), (29) and (30). For example, the electric fields for the TM case can be written as

$$\vec{E}_s = -E_0 \sum_{n=0}^{\infty} \varepsilon_n (-i)^n b_{nI} H_n^{(1)}(\rho) \cos n\varphi \hat{e}_z \tag{34}$$

$$\vec{E}_j = E_0 \frac{k_j}{k} \sum_{n=0}^{\infty} \varepsilon_n (-i)^n [d_n^{(j)} J_n(m_j x_j) + f_n^{(j)} Y_n(m_j x_j)] \cos n\varphi \hat{e}_z \tag{35}$$

and for TE case

$$\vec{E}_s = E_0 \sum_{n=0}^{\infty} \varepsilon_n (-i)^{n+1} a_{nII} \Big[n \frac{H_n^{(1)}(\rho)}{\rho} \sin n\varphi \hat{e}_r$$
$$+ H_n^{(1)'}(\rho) \cos n\varphi \hat{e}_\varphi \Big] \tag{36}$$

$$\vec{E}_j = -E_0 \frac{k_j}{k} \sum_{n=0}^{\infty} \varepsilon_n (-i)^n \Big\{ \frac{n \sin n\varphi}{m_j x_j} [c_n^{(j)} J_n(m_j x_j) + g_n^{(j)} Y_n(m_j x_j)] \hat{e}_r$$
$$+ \cos n\varphi [c_n^{(j)} J_n'(m_j x_j) + g_n^{(j)} Y_n'(m_j x_j)] \hat{e}_\varphi \Big\} \tag{37}$$

where

$$\varepsilon_n = \begin{cases} 2 & \text{for } n = 1, 2, 3, \dots \\ 1 & \text{for } n = 0 \end{cases} \tag{38}$$
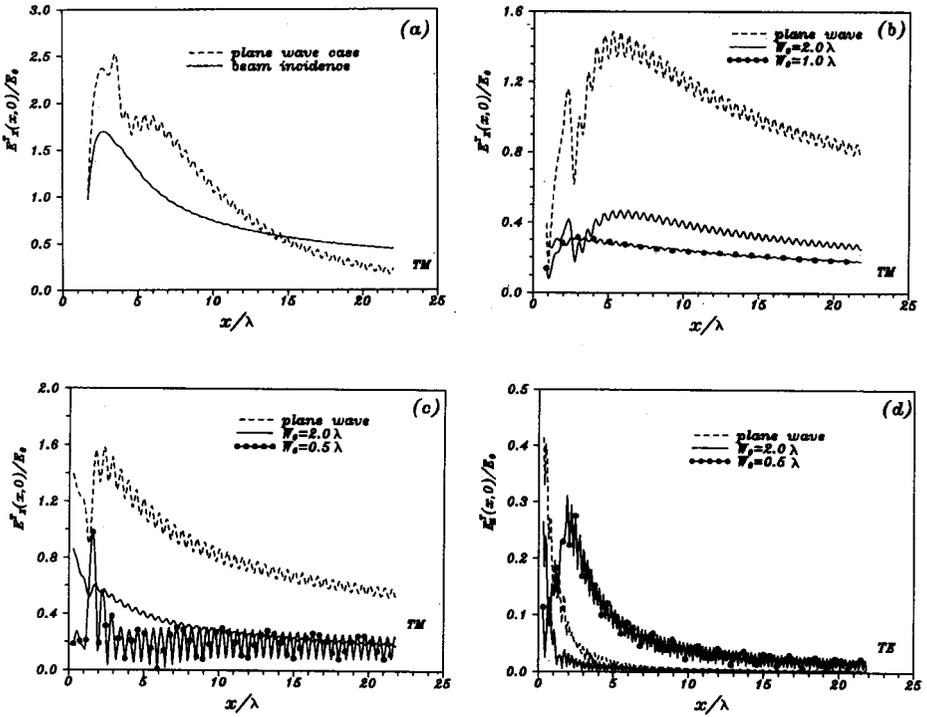
Figure 4. Amplitude of scattering field in the forward direction.

The internal coefficients $c_n^{(j)}$, $d_n^{(j)}$, $g_n^{(j)}$, $f_n^{(j)}$ can also be obtained from the recursive algorithms which are published in our another paper [4]. The corresponding components of magnetic field can also be obtained from Maxwell equations.

In order to check the validity of scattering field, accurate numerical computations have been performed. In Fig. 4, the propagation behavior of the scattering from the cylinder is pictured. In Fig. 4(a), the amplitude of scattering field (TM case) from a homogeneous cylinder is plotted versus x/λ at $y_0 = 0$ for $W_0 = 4.05\lambda$. $x_0/\lambda = 10.0$, the relative permittivity $\varepsilon = 1.46$ and the radius of this cylinder $a/\lambda = 1.74$. It is found that the scattering pattern we obtained is just consistent with the one given by reference [9], but there exists some differences in amplitude for the plane wave case.

Fig. 4(b) depicts numerical result of the electric field along x-axis for a two layers dielectric cylinder (TM case) for $y_0/\lambda = 1.0$, $x_0/\lambda = 2.0$, $kr_1 = 5.0$, $kr_2 = 5.5$, and the relative permittivity $\varepsilon_1 = 1.0$, $\varepsilon_2 = 2.56 + 0.1024i$, respectively. It is seen clear that the amplitude of the plane wave incident is larger than that of Gaussian beam incident, and it is found that the amplitude depends on the beam waist W_0.

In many applications, the scattering of inhomogeneous or multilayered cylinders are of primary interest. Our approach produces accurate results which are displayed in Fig. 4(c) and Fig. 4(d) for TM and TE beam incident respectively. The cylinder has an outer radius $a = 0.3\lambda$, $y_0/\lambda = 1.0$, $x_0/\lambda = 2.0$, and the change of the relative permittivity with the radius depends on the relation $\varepsilon_r = 2 - (r/a)^2$. This relation is approximated by 80-layer discrete cylinder.

After obtaining the scattering coefficients from (29) and (30), the scattering widths can be expressed as [13]

$$\sigma_{TM}(\varphi) = \frac{4}{k} \left| \sum_{n=-\infty}^{\infty} (-1)^n \varepsilon_n b_{nI} \cos(n\varphi) \right|^2 \tag{39}$$

$$\sigma_{TE}(\varphi) = \frac{4}{k} \left| \sum_{n=-\infty}^{\infty} (-1)^n \varepsilon_n a_{nII} \cos(n\varphi) \right|^2 \tag{40}$$

Fig. 5((a)–(d)) illustrate the angular distribution of the normalized scattering widths from (39) and (40). The parameters correspond to those of Fig. 4((a)–(d)). It is also found that the scattering width of different cylinders for the Gaussian beam and the plane wave incidence has a similar form, but the amplitude of the pattern for the plane wave is larger than that for the Gaussian beam. For example, in Fig. 5(b), it is shown that when the beam waist increases, the results will gradually approach to that of the plane wave case. As larger the beam waist is, closer result for the Gaussian beam and the plane wave incidence is. The results of the plane wave case are in agreement with the results given by G. T. Ruck [13]. Consequently, our method built with the iterative algorithm is validated.

5. CONCLUSION

We have studied the scattering of an off-axis 2D Gaussian beam by a multilayered cylinder. The beam shape coefficients are obtained in a simple expression with first-order approximation. A new algorithm
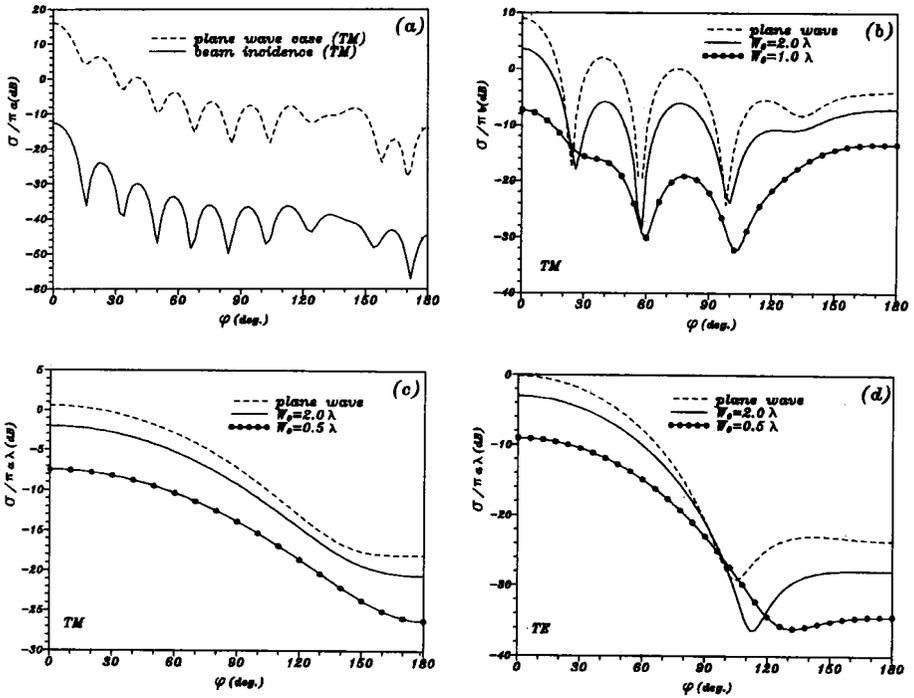
Figure 5. The angular distribution of the normalized scattering widths.

to predict the interaction between electromagnetic wave and a multilayered cylinder with its associated numerical procedures have been presented. The computational domain, which is implemented as a FORTRAN LF90 code, is increased by several magnitude orders, both in size parameter and in the number of layers for a given size. Numerical results for the scattering fields of different multilayered cylinders, including near and far fields, are successfully obtained. When the radius of the cylinder is much smaller than the size of the Gaussian beam, the plane wave scattering solution is obtained as the limit case. The results getting from our method has been verified with a good accuracy and found to be more widely used.

ACKNOWLEDGMENT

REFERENCES

1. Kong, J. A, *Theory of Electromagnetic Wave,*, John Wiley & Sons, 1986.
2. Yuan, X., D. R. Lynch, and J. W. Strohbehn, "Coupling of finite element and moment method for electromagnetic scattering from inhomogeneous objects", *IEEE Tran. AP.,* Vol. 38, 386–393, 1990.
3. Wu, Z., and Y. Wang, "Electromagnetic scattering for multilayered sphere : recursive algorithms", *Radio Science,* Vol. 26, 1393–1401, 1991.
4. Wu, Z., and L. Guo, "Internal and external electromagnetic fields for multilayered cylinders at normal incidence", *ACTA ELECTRONICA SINICA (in Chinese),* Vol. 23, 114–116, 1995.
5. Bussey, H. B., and J. H. Richmond, "Scattering by a lossy dieletric circular cylindrical multilayers : Numerical values", *IEEE Tran. AP.,* Vol. 23, 723–725, 1975.
6. Morita, N., et al., " Scattering of a beam wave by a spherical object", *IEEE Tran. AP.,* Vol. 16, 724–727, 1968.
7. Alexopoulos, N. G. et al., "Scattering of waves with normal amplitude distribution from cylinders", *IEEE Tran. AP.,* Vol. 20, 216–217, 1972.
8. Kojima, T. et al., "Scattering of an offset two dimentional Gaussian beam wave by a cylinder", *J. Appl. Phys.,* Vol. 50, 41–46, 1979.
9. Kozaki, S., "Scattering of a Gaussian beam by a homogeneous dielectric cylinder", *J. Appl. Phys.,* Vol. 53, 7195–7200, 1982.
10. Zimmermann, E., R. Dandliker, and N. Souli, "Scattering of an of off-axis Gaussian beam by a dielectric cylinder compared with a rigorous electromagnetic approach", *J. Opt. Soc. Am. A,* Vol. 12, 398–403, 1995.
11. Yokota, M., and T. Takenaka et al., "Scattering of Hermite-Gaussian beam mode by parallel dielectric circular cylinders", *J. Opt. Soc. Am. A,* Vol. 3, 580–586, 1986.
12. Wu, X., and R. Wei, "Scattering of a Gaussian beam by an anisotropic material coated conducting circular cylinder", *Radio Science,* Vol. 30, 403–411, 1995.
13. Rucketal, G. T., *Radar Cross Section Handbook,* Plenum, New York, 1970.